Applied Catalysis B: Environmental 248 (2019) 95–107

Contents lists available at ScienceDirect

Applied Catalysis B: Environmental

journal homepage: www.elsevier.com/locate/apcatb

Electrosynthesis of hydrogen peroxide using modified gas diffusion electrodes (MGDE) for environmental applications: Quinones and azo compounds employed as redox modifiers

Juliana Moreira[a], Verônica Bocalon Lima[a], Lorena Athie Goulart[a], Marcos R.V. Lanza[a,b,*]

[a] Institute of Chemistry of São Carlos, São Paulo University, Avenida Trabalhador São Carlense 400, São Carlos, SP, 13566-590, Brazil
[b] National Institute of Alternative Technologies for Detection, Toxicological Evaluation and Removal of Micropollutants and Radioactive Substances (INCT-DATREM), Institute of Chemistry, Unesp, Araraquara, 14800-900, SP, Brazil

ARTICLE INFO

Keywords:
Electrosynthesis of hydrogen peroxide
Oxygen reduction reaction
Gas diffusion electrode
Redox organic compounds modifiers
Carbon black -based electrodes

ABSTRACT

Although the electrosynthesis of hydrogen peroxide (H_2O_2) using gas diffusion electrodes (GDE) is a viable option for the production of this oxidizing agent in advanced oxidation processes (AOP) for wastewater treatment, the quest for more efficient electrodes is still regarded a matter of great importance in this area. The present study sought to investigate different redox organic compounds employed as modifiers of carbon black Printex L6 (CP) with the aim of increasing H_2O_2 production using carbon-based electrodes. Varying amounts of the modifiers, including Sudan Red 7B (SR7B), methyl-p-benzoquinone (MPB), anthraflavic acid (AA) and anthraquinone-2-carboxylic acid (A2CA), were added to carbon black, where the electrochemical activity was studied by applying a microporous catalyst layer on a rotating ring-disk electrode (RRDE). The materials containing 0.5% of SR7B and 5.0% of MPB increased the current efficiency for the electrogeneration of hydrogen peroxide to 86.2% and 85.5%, respectively, compared to 82.8% obtained for unmodified carbon. Carbon Printex L6 gas diffusion electrodes modified with 0.5% of SR7B were studied and the following results were obtained: the application of current density of 75 mA cm^{-2} led to the production of 1020.1 mg L^{-1} of H_2O_2, with an energy consumption of 118.0 kW h kg^{-1}, apparent kinetic constant of 37.34 mg L^{-1} min^{-1} and current efficiency of 17.87%. Conversely, the use of GDE with unmodified carbon resulted in the production of relatively less quantity of H_2O_2 which amounted to 717.3 mg L^{-1}, with more energy consumption of 168.5 kW h kg^{-1}, lower apparent kinetic constant of 21.41 mg L^{-1} min^{-1} and lower current efficiency of 12.57%. Based on these results, carbon Printex L6 GDE modified with 0.5% of Sudan Red 7B is seen as a suitable alternative for the production of high amounts of H_2O_2 which can be applied in advanced oxidation processes in acidic medium.

1. Introduction

It is quite worrying to note that despite the fact that only a small fraction of the water on planet Earth is available for human consumption, this limited resource has for long been suffering from the action of human pollution and has been extensively used in a wasteful fashion with complete disregard for its limited nature [1,2]. In the face of the increasing degree of water pollution, municipal water treatment plants are found to be generally unprepared to help get rid of hazardous pollutants such as emerging contaminants in water that pose serious threats to both human life and the environment [3–5]. These pollutants are found in trace concentrations ranging from ng L^{-1} to μg L^{-1}, thus making their detection, quantification and treatment in wastewater greatly difficult [6,7]. In Brazil, only 28.5% of municipalities have sewage treatment plants, so chances of recalcitrant molecules finding their way into drinking water remain high [8,9].

The application of advanced oxidative processes (AOP) stands as an alternative to the classic treatment processes [10]. The AOPs are based on the generation of highly reactive species, such as hydroxyl radicals (•OH) in aqueous phase, derived from oxidant species like hydrogen peroxide (H_2O_2), which oxidize pollutants [11,12]. *In situ* production of hydrogen peroxide gained importance as a result of the risks associated with transportation, handling and storage of this compound [13,14]. In addition, the concentration of hydrogen peroxide is a critical parameter when it comes to the application of AOPs. This is mainly attributed to the fact that the compound is quickly consumed during the generation of hydroxyl radicals. Apart from that, the addition of high concentrations in reaction medium leads to the reaction between hydroxyl

* Corresponding author at: Institute of Chemistry of São Carlos, São Paulo University, Avenida Trabalhador São Carlense 400, São Carlos, SP, 13566-590, Brazil.
E-mail addresses: juliana.moreira@usp.br (J. Moreira), marcoslanza@usp.br (M.R.V. Lanza).

https://doi.org/10.1016/j.apcatb.2019.01.071
Received 1 August 2018; Received in revised form 24 January 2019; Accepted 27 January 2019
Available online 29 January 2019
0926-3373/

radicals with H_2O_2, generating hydroperoxyl radicals ($HO_2^{\cdot}$) known to be characterized by lower oxidizing power, which tends to compromise the efficiency of these processes [15,16].

Hydrogen peroxide can be produced electrochemically by oxygen reduction reaction (ORR). The two main mechanisms that involve the production of hydrogen peroxide are as follows: direct or 4-electron mechanism in which water is produced; and hydrogen peroxide mechanism or 2-electron mechanism where hydrogen peroxide is produced [17–20]. These reactions depend on the applied overpotential and the surface of the electrode [21]. ORR is generally limited by oxygen supply due to low solubility of this gas in aqueous medium. However, the use of highly porous electrodes with a large active area, such as gas diffusion electrodes (GDE), facilitates the diffusion of gaseous reagents to the catalytic sites, eliminating the influence of mass transport of oxygen [17,22–26].

The use of highly porous gas diffusion electrodes and modifiers, such as quinones, azobenzenes and metallic phtalocyanines immobilized to carbon matrix of GDE contributes toward the improvement of oxygen supply in solution and the decrease of overpotentials required for ORR, apart from enhancing the generation of H_2O_2 [23,27,28]. Carbon is a catalytic material widely used as electrode (cathode) for ORR via two electrons aimed at the generation of H_2O_2. Its ample use as catalytic material can be attributed to its large surface area, corrosion resistance and low price. Carbon black pigment Printex L6 has been used in ORR electrodes due to the high oxygen content and greater hydrophilicity of this material. These properties make the material suitable for H_2O_2 generation [29,30].

Different mechanisms for ORR have been proposed in the literature, where hydrogen peroxide is generated on carbon electrodes with the participation of a strong interaction of oxygen with functional groups on carbon surface, such as SO, NO, quinones and carboxylic acids [31].

Quinones can be used as carbon modifiers in order to enhance the generation of hydrogen peroxide. In acid medium, it is observed the reduction reaction of quinones as shown in Eq. (1). In the presence of oxygen, the reaction may continue to generate hydrogen peroxide based on Eq. (2) [32]:

$$Q + 2H^+ + 2e^- \rightleftharpoons QH_2 \quad (1)$$

$$QH_2 + O_2 \rightarrow Q + H_2O_2 \quad (2)$$

The presence of quinones and azo compounds on carbon surface can increase the generation of hydrogen peroxide as a result of the reduction of functional groups in quinones and azo compounds structures. In addition, modifiers have also been studied aiming at the reduction of overpotentials required for ORR to occur [22,33]. Modifiers are organic or inorganic compounds that have been investigated along with the application of the microporous layer technique on rotating ring-disk electrodes (RRDE). Some of these modifiers have already been applied to GDE. Among the most studied inorganic modifiers include Ta_2O_5, Nb_2O_5, Fe_3O_4, zirconia nanoparticles, ZrO_2, cerium oxide, V_2O_5 and tin and nickel composites [34–42]. The most commonly investigated organic modifiers include metal phthalocyanines, such as copper (II), cobalt (II) and iron (II) phthalocianines; porphyrins like cobalt tetramethoxyphenyl porphyrin; and quinones including tert-butyl anthraquinone, 2-ethylanthraquinone and 2-tert-butylanthraquinone [14,22–25,27,28,43–45].

Although most of the modifiers employed in the generation of H_2O_2 are inorganic modifiers, great results have been achieved with the application of organic modifiers. This shows the remarkable potential of organic modifiers. In addition, while organic modifiers can be physically mixed with carbon, the inorganic ones need to be synthesized separately, and this requires higher temperatures and longer time to obtain the modified material.

The present work sought to study the quinones, namely, methyl-p-benzoquinone (MPB), anthraflavic acid (AA) and anthraquinone-2-carboxylic acid (A2CA) and the azo compound Sudan Red 7B (SR7B) as organic modifiers of Printex L6 carbon (CP). These compounds were chosen because they exhibited different groups of donors and electron withdrawals, allowing an investigation of the redox processes of each modifier and their correlation with the generation of hydrogen peroxide.

2. Materials and methods

2.1. Study of the oxygen reduction reaction (ORR)

The evaluation of the electroactivity of the modifiers for hydrogen peroxide production was performed by applying a microporous layer of the materials investigated in this study on a rotating ring-disk electrode.

The catalysts materials were prepared as described in the literature [23] by physical mixture of carbon Printex L6 (acquired from Evonik Brasil Ltd.) and the modifiers including 95% of Sudan Red 7B, 98% of methyl-p-benzoquinone, 90% of anthraflavic acid and 98% of anthraquinone-2-carboxylic acid (obtained from Sigma Aldrich). The proportions (w/w) employed were: 0.5%, 1.0%, 1.5%, 3.0% and 5.0% for Sudan Red 7B and methyl-p-benzoquinone; 0.5%, 1.0%, 1.5%, 2.0%, 2.5%, 3.0% e 5.0% for anthraflavic acid and anthraquinone-2-carboxylic acid.

The mixtures of carbon Printex L6 (CP) and methyl-p-benzoquinone (MPB); CP and anthraflavic acid (AA); or CP and anthraquinone-2-carboxylic acid (A2CA) were dispersed in 20 mL of isopropyl alcohol P.A. 99.5% (Quimis). The mixture of CP with Sudan Red 7B (SR7B) was dispersed in 10 mL of isopropyl alcohol P.A. 99.5% (Quimis) along with 10 mL of acetone. The dispersions were dried in drying chamber at 80 °C, 45 °C and 70 °C for Sudan Red 7B, methyl-p-benzoquinone, and for both anthraflavic acid and anthraquinone-2-carboxylic acid, respectively, for 4 h. The reference material used for ORR which promoted the production of water was carbon-supported platinum catalyst (Pt/C) at 20% (w/w) from E-TEK (BASF).

The microporous layers were obtained by dispersing 1.0 mg of carbon Printex L6, carbon Printex L6 with modifiers and Pt/C in 1.0 mL of ultrapure water. An aliquot of 25 µL of the dispersion was deposited on the disk of the RRDE with the aid of a micropipette and the film was dried at N_2 flow of 1.0 mL min^{-1}.

A three-electrode electrochemical cell was employed which consisted of platinum as counter electrode, Ag/AgCl (saturated) as reference electrode and RRDE as working electrode. To conduct voltammetry measurements, we employed Autolab model PGSTAT302 N potentiostat equipped with a rotating ring-disk electrode system and RRDE model AFE7R9GCPt from Pine Research Instrumentation with collection coefficient of 0.38.

All the cyclic and linear sweep voltammetry measurements were carried out using K_2SO_4 0.1 mol L^{-1} solution under pH 3 adjusted with H_2SO_4 solution. For the cyclic voltammetry, the electrolyte was saturated with N_2 and the measurements were performed at a scan rate of 50 mV s^{-1}. For the linear sweep voltammetry, the electrolyte was saturated with O_2 and the measurements were carried out at a scan rate of 5.0 mV s^{-1} with rotation velocity ranging from 100 to 2500 rpm and ring potential at +1.0 V.

2.2. Characterization of electrocatalysts materials

Contact angles for the best proportion of each material obtained from the experiments with RRDE were determined using an angle meter from Attension Theta. Microporous layers of carbon Printex L6 and carbon Printex L6 containing the modifiers were produced on the RRDE disc and a drop of ultrapure water of 3.0 µL was poured on the microlayer. Images of the drop of water on the surface of the microlayer were acquired and the average contact angles were calculated based on the contact angle measurements between the drop of water and the surface of the microlayer.

Transmission electron microscopy analyses were performed using

the following: TEM JEOL, model JEM 2100, with a thermionic electron source LaB_6 at a voltage of 200 kV, a digital camera Gatan 2k on a scale of 200 nm with magnification of 200,000 and processing software Gatan Microscopy Suite 3. The samples were prepared via the dispersion of the materials (carbon Printex L6 and carbon Printex L6 modified with 0.5, 1.0, 1.5 and 3.0% of Sudan Red 7B in isopropyl alcohol in the ratio 1:10000). After that, a droplet of the dispersion was pipetted over a copper grid covered with a carbon film, with 300 mesh acquired from Electron Microscopy Sciences (CF300-CU). The dispersion was then dried in air for 90 min and was subsequently placed in a vacuum desiccator made of glass.

2.3. Electrogeneration of H_2O_2 on GDE

Based on the results obtained from the RRDE experiments, carbon Printex L6 GDE and carbon Printex L6 GDE modified with 0.5% of Sudan Red 7B were used to conduct electrolysis aiming at the production of H_2O_2 *in situ*.

The catalytic mass was prepared as described in the literature [27]. Sudan Red 7B was added in a proportion of 0.5% (w/w) to carbon Printex L6, and isopropyl alcohol and acetone were then added to the mixture until it became homogeneous. After that, the mixture was dried at 100 °C. Thereafter, 40 g of the dried mixture (for modified GDE) or 40 g of carbon Printex L6 (for unmodified GDE) were dispersed in ultrapure water. Subsequently, 16.7 g of polytetrafluorethylene (PTFE) solution (DuPont) were added in a proportion of 20% relative to the total mass of carbon and kept under stirring. The suspension was filtered under vacuum to remove water and was then dried at 120 °C [46].

A quantity of mass regarded sufficient to obtain an electrode of 8 g was pressed between two metal screens in the external sides of the GDE in a steel mold under heating of 220 °C, 11.5 ton for 2 h. An electrochemical cell with a single compartment made of glass was employed here. The following were placed within the cell: a counter electrode composed of titanium covered with platinum of 70.5 cm^2, a reference electrode of Ag/AgCl (saturated) and a mechanical shaker. The GDE was also placed at the bottom of the cell. The electrochemical cell was kept at 20 °C by passing water around the cell at this temperature. 250 mL of K_2SO_4 0.1 mol L^{-1} (employed as electrolyte) were employed under pH 3 adjusted with H_2SO_4 solution.

All the experiments were performed using a bipotentiostat - Autolab model PGSTAT 302 N, with a high current unit of BSTR-10 A. The electrolysis was conducted at 10, 20, 50, 75, 100 and 150 mA cm^{-2} for 90 min, after saturating the electrolyte with O_2 for 40 min and maintaining it at 0.3 bar during the experiments.

Aliquots of 0.5 mL were taken before the electrolysis (time 0), and during the experiments. The aliquots were added to 4.0 mL of ammonium molybdate solution $(NH_4)_6Mo_7O_{24}$ at $2{,}4.10^{-3}$ mol L^{-1} in 0.5 mol L^{-1} of H_2SO_4. The H_2O_2 in that solution produces a yellow complex peroxymolybdate that adsorbs wavelength light at 350 nm. The quantification was obtained in a spectrophotometer Cary 50 from Varian and calculated according to the Lambert-Beer equation.

3. Results and discussion

3.1. Study of the oxygen reduction reaction (ORR)

Cyclic voltammograms (depicted in Fig. 1(a)) for carbon Printex L6 modified with methyl-p-benzoquinone (MPB) showed oxidation and reduction peaks at 0.3 and 0.2 V, respectively. These peaks are probably related to carbonyl groups, where −C═O groups are reduced to −C−OH and are thereafter oxidized to −C═O. Regions between 1.0 and 0.4 V and 0.1 and −0.8 correspond to regions without faradaic contribution. When these values are compared with different percentages of the modifiers, the values are almost the same; this implies the existence of reproducibility between the experiments. The slight change in peaks observed between the microporous layers can be attributed to the formation of agglomerates which may have changed the resistivity of the layers. The increase in the amount of modifier did not necessarily lead to an increase in peak current; this may likewise be attributed to the presence of agglomerates. The methyl groups pertaining to these modifiers act as weak activating groups of the ring that can increase the electron density in the ring. In the case of the −C═O groups, this consequently facilitates their reduction to −C−OH [47].

For the materials containing anthraquinone-2-carboxylic acid (A2CA), the microlayers containing 2.5%, 3.0% and 5.0% of the modifier were impossible to be used because the materials did not undergo dispersion in ultrapure water nor in isopropyl alcohol even after 50 min in ultrasound. As a result, the following percentages of the modifier were subjected to investigation: 0.5, 1.0, 1.5 and 2.0%. Voltammograms in Fig. 1(b) show that the quinone has both an oxidation peak and a reduction peak close to -0.2 and -0,3 V, respectively; these peaks are possibly related to either the carbonyl group or the carboxyl group (−COOH), and may also be associated with an oxidation peak at 0.1 V. Interestingly, in regions without faradaic contributions, no change was observed in the current values; this is indicative of reproducibility of the experiments as noted in the case of metyl-p-benzoquinone. The carboxyl group can act as a moderate deactivating group of the ring that can reduce the electron density in the ring, making it more difficult to reduce the carbonyl groups and facilitating the re-oxidation of their reduced form [47].

The materials with anthraflavic acid (AA) showed in Fig. 1(c) exhibited two peaks of oxidation at −0,3 and 0,0 V and two peaks of reduction at −0,1 and −0,4 V. This can possibly be attributed to the presence of quinone and hydroxyl groups in the structure of anthraflavic acid. No variation was observed in the current values in regions without faradaic contributions; this again implies the existence of reproducibility. Materials containing 3.0 and 5.0% of this modifier failed to undergo dispersion. As a result, the materials containing 0.5, 1.0, 1.5, 2.0 and 2.5% of the modifier were investigated. It is important to emphasize that this modifier has 2 hydroxyl groups, which are strong activating groups of the rings that can facilitate the reduction of the carbonyl groups [47].

Cyclic voltammograms in Fig. 1(d) for the materials containing azo compound Sudan Red 7B (SR7B) showed two oxidation peaks at 0.2 and -0.2 V and two reduction peaks at 0.15 and −0.2 V. This can be attributed to the presence of two azo groups (−N═N−) in the structure of this compound that can be reduced to HN−NH [47]. In regions without faradaic contribution, variation was observed in the current values, mainly for the material containing 5.0% of the modifier. This behavior can be associated with the formation of agglomerates in the microporous layer with the exposure of the vitreous carbon surface of the electrode, which contributes to a decline in the current values.

Linear sweep voltammograms were obtained for each microporous layer with electrode rotation speed ranging from 100 to 2500 rpm. The results obtained for the electrode with rotation speed of 900 rpm were used for comparison purposes. Fig. 2 shows the linear sweep voltammograms for the best proportion of each modifier and for carbon Printex L6 (CP). For the voltammograms related to the materials containing different amounts of modifiers, the currents between 0.4 and −0.1 V were found to be associated with the capacitive currents of the microporous layers. A mixed control is noted between −0.1 and −0.6 V, where an increase in potential generates an increase in current, and reactions are found to be controlled by charge and mass transport. Finally, between −0.6 and −0.8 is observed the existence of diffusional control region, in which the reactions depend on mass transport. Here, even with an increase in potential, no increase is observed in the current values.

The linear sweep voltammograms showed that there is a variation in the disk currents for different microporous layers. This implies that depending on the amount of modifier added to the carbon matrix, different mechanisms of reaction may have occurred. Besides that, no changes were observed in the starting potential of the oxygen reduction

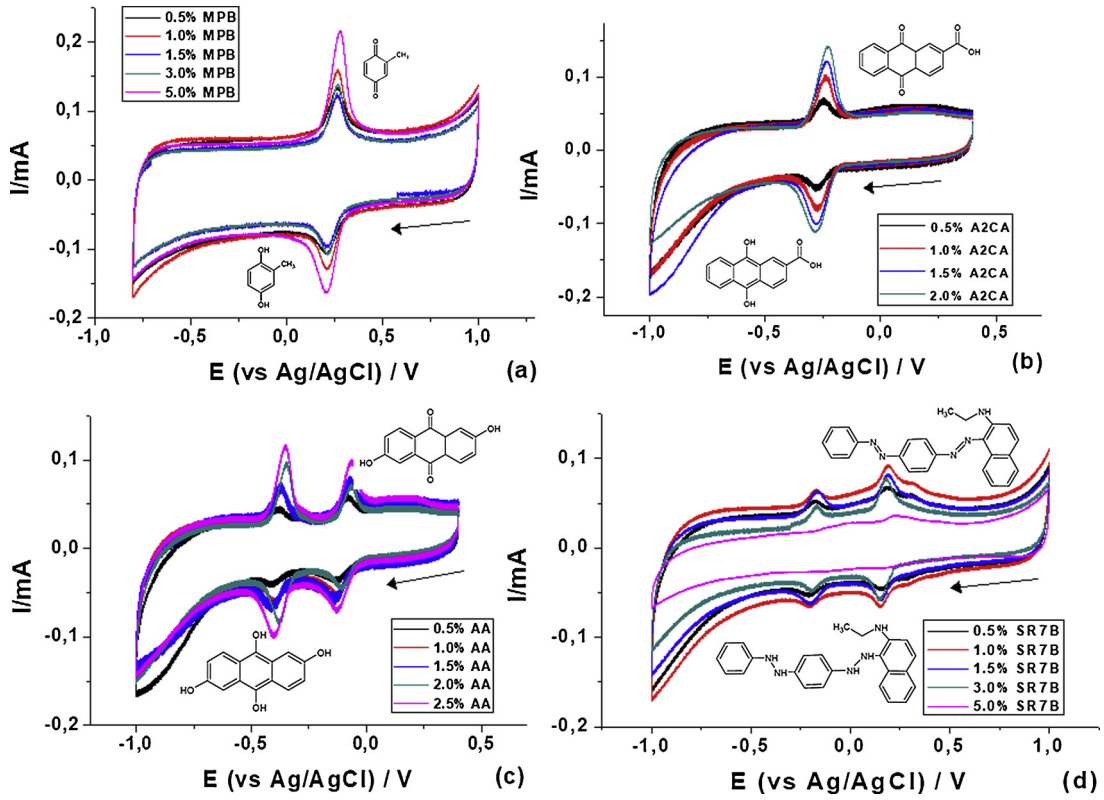

Fig. 1. Cyclic voltammograms for each microporous layer containing different amounts of methyl-p-benzoquinone, MPB (a) anthraquinone-2-carboxylic acid, A2CA (b) anthraflavic acid, AA (c) and Sudan Red 7B, SR7B (d). The structures of each molecule are shown in the graphs. The scan rate employed here was 50 mV s^{-1}. The electrolyte employed was 0.1 mol L^{-1} of K_2SO_4 at pH 3 and saturated with N_2. The arrow indicates the direction of potential scanning.

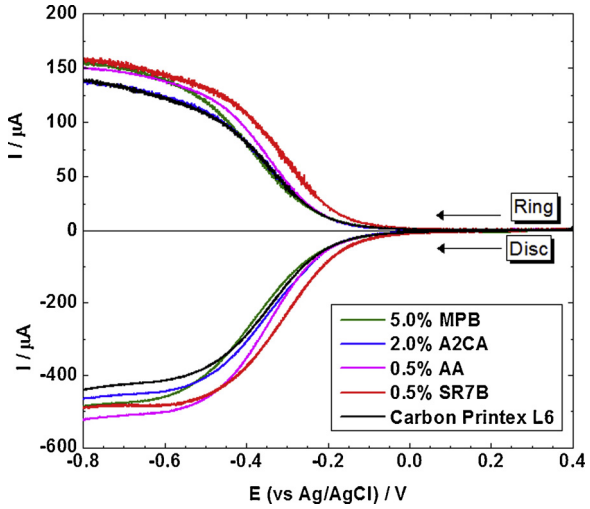

Fig. 2. Linear sweep voltammograms for different proportions of each modifier that most increased the ring current values in comparison to carbon Printex L6. Scan rate was 5 mV s^{-1}. The electrolyte employed here was 0.1 mol L^{-1} of K_2SO_4 at pH 3 and saturated with O_2. The arrow indicates the direction of potential scanning.

reaction in the disk for any of the materials containing modifiers in relation to the carbon Printex L6 (CP). In view of that, none of these materials is seen to lead to a reduction in energy consumption through the effect of the reduction of overpotential necessary for the oxygen reduction reaction. Thus, by the effect of the reduction of the overpotential, the closer the overpotential is to 0.0 V, the lower is the energy consumed. The material containing 5.0% of Sudan Red 7B led to a shift to more negative potentials that could lead to an increase in energy consumption. Furthermore, the regions are also found to have shifted to more negative potentials; this can be attributed to the difficulty encountered in the dispersion of this material and agglomerates may have been formed as a result.

The ring currents for the materials containing 5.0% (showed in Fig. 2), 3.0 and 1.5% of methyl-p-benzoquinone (MPB) were higher than those for carbon Printex L6. The materials containing 0.5 and 1.0% of MPB presented relatively lower ring currents compared to carbon. In this sense, greater mass additions of this modifier resulted in higher generation of H_2O_2.

The ring current values for the materials containing 0.5, 1.0, 1.5 and 2.0% of anthraquinone-2-carboxylic acid (A2CA) were relatively lower than the current values observed for carbon Printex L6. In this sense, this modifier seems to be incapable of increasing H_2O_2 generation. The material containing 2.0% of A2CA, which was found to be the closest to carbon Printex L6, is shown in Fig. 2.

The material containing 0.5% of anthraflavic acid (AA) presented ring current values higher than the currents observed for carbon Printex L6, as shown in Fig. 2. This indicates that the addition of this compound to carbon resulted in an increase in H_2O_2 generation. The materials with greater proportions of this compound exhibited relatively lower ring currents.

In similar observations, the ring currents were found to be higher for materials containing 0.5%, 1.0 and 1.5% of Sudan Red 7B (SR7B) compared to the currents observed for carbon Printex L6. In view of that, it is possible to infer that the use of this modifier tends to increase H_2O_2 generation. In addition, the ring currents in the diffusional control region were also found to be higher; this implies that the use of the aforementioned amounts (0.5, 1.0, and 1.5%) of the modifier helps to increase H_2O_2 generation. The materials with 5.0 and 3.0% presented the lowest current values, hence, lower amounts of the modifier resulted in a greater production of H_2O_2.

Based on the results obtained from the linear sweep voltammetry for

Table 1
Current efficiency for hydrogen peroxide electrogeneration (% H_2O_2) and total number of electrons exchanged (n_t) for carbon Printex L6, Pt/C and materials containing the modifiers. The data below are related to the potential of −0.55 V for materials containing the modifiers as well as for carbon Printex L6; and the potential of 0.25 V for Pt/C.

		Pure	0.5%	1.0%	1.5%	2.0%	2.5%	3.0%	5.0%
CP	$\%H_2O_2$	82.8	–	–	–	–	–	–	–
	n_t	2.4	–	–	–	–	–	–	–
MPB	$\%H_2O_2$	–	82.4	84.8	85.3	–	–	84.9	85.5
	n_t	–	2.3	2.3	2.3	–	–	2.3	2.3
A2CA	$\%H_2O_2$	–	79.4	79.9	81.4	83.8	–	–	–
	n_t	–	2.4	2.4	2.4	2.3	–	–	–
AA	$\%H_2O_2$	–	83.3	80.7	82.4	81.1	82.8	–	–
	n_t	–	2.3	2.4	2.3	2.4	2.3	–	–
SR7B	$\%H_2O_2$	–	86.2	85.2	83.8	–	–	82.2	73.9
	n_t	–	2.3	2.3	2.3	–	–	2.3	2.5
Pt/C	$\%H_2O_2$	0.3	–	–	–	–	–	–	–
	n_t	3.9	–	–	–	–	–	–	–

each microporous layer, it was calculated the current efficiency for hydrogen peroxide electrogeneration using the following equation [44]:

$$\%H_2O_2 = \frac{200\frac{ir}{N}}{id + \frac{ir}{N}}$$

where i_r is the ring current, i_d is the disk current, and N is the collection coefficient. The tendency of the mechanism for reaction via 2 or 4 electrons was also calculated using the equation below [44]:

$$nt = \frac{4|id|}{|id| + \frac{ir}{N}}$$

The current values used to perform the calculations were obtained from the linear sweep voltammograms at 900 rpm which corresponded to the potential at the beginning of the diffusional control.

The values calculated relative to the current efficiency for hydrogen peroxide electrogeneration ($\%H_2O_2$) along with the total number of electrons exchanged (n_t) in the reaction for carbon Printex L6, Pt/C and materials containing the modifiers are presented in Table 1. The values obtained for carbon Printex L6 were used as a reference for oxygen reduction reaction via 2 electrons that lead to H_2O_2 generation, while those values related to Pt/C were used as a reference for reaction via 4 electrons with H_2O generation. The experiments were conducted in triplicate and the standard deviation value obtained was 2.5% for % H_2O_2.

The materials containing 1.5, 3.0 and 5.0% of methyl-p-benzoquinone (MPB) presented a greater current efficiency compared to carbon Printex L6, when the standard deviation is taken into consideration. Those materials containing 0.5; 1.0 and 1.5% of anthraquinone-2-carboxylic acid (A2CA) presented a decrease in current efficiency compared to carbon Printex L6. Moreover, although an increase in current efficiency was observed for the materials containing 2.0% of A2CA, the increase was not significant when the standard deviation is taken into account. For the materials containing anthraflavic acid (AA), a relatively higher decrease in current efficiency was noted in comparison to carbon for all the different percentages of the modifier employed except for 0.5% which recorded an increase in current efficiency. However, this increase (for the material containing 0.5% of AA) was not significant when the standard deviation is taken into account. Finally, materials containing 0.5, 1.0 and 1.5% of Sudan Red 7B (SR7B) presented an increase in current efficiency, though when one takes the standard deviation into account only materials with 0.5% presented a significant increase in current efficiency when it comes to H_2O_2 generation.

With regard to the total number of electrons transferred (or exchanged) in the reaction, the standard deviation for the experiments conducted in triplicate was 0.06; as such, it is possible to infer that both carbon Printex L6 and all the materials with modifiers have the tendency for reaction via 2 electrons.

In this context, materials containing 5.0% of methyl-p-benzoquinone and 0.5% of Sudan Red 7B exhibited an increase in H_2O_2 production compared to carbon and can, thus, be applied in gas diffusion electrodes. Clearly, these reported effects can be better evaluated by applying the modifiers in gas diffusion electrodes. This is because by using these electrodes one can possibly detect and quantify the concentration of H_2O_2 obtained.

The improvements in H_2O_2 electrogeneration observed in materials containing Sudan Red 7B can be attributed to the presence of azo groups in the molecules of the modifier that can participate in ORR reaction. An increase in H_2O_2 production was observed in a study that employed azobenzene as a modifier of carbon Printex L6. The authors showed that the azo group of this molecule is reduced by two electrons and receives two protons; oxygen is then reduced to superoxide anion which may undergo disproportionation to H_2O_2 [27]. In this sense, in the case of Sudan Red 7B, the azo groups may undergo reduction; and the oxygen molecule (O_2) is reduced to H_2O_2 when it comes nearer, while the azo groups are oxidized again.

Methyl-p-benzoquinone also presented a relatively higher H_2O_2 electrogeneration. This result can be attributed to the methyl group in its structure which can activate the ring, leading to the reduction of the carbonyl group. In the presence of O_2, the carbonyl group is oxidized while the O_2 is reduced to H_2O_2. Since the activation from the methyl group is weak, the molecule can easily return to its oxidized form.

For other quinones like tert-butyl anthraquinone, the understanding, according to the literature, is that ORR is associated with an electrochemical/chemical mechanism, where quinone is reduced in a single step with the transfer of two electrons and two protons. In the second step, quinone undergoes an auto-oxidation in the presence of molecular oxygen, releasing two protons and two electrons. These released electrons and protons subsequently reduce oxygen in the third step, generating H_2O_2 in acid medium [23]. This is similar to what is observed in the case of methyl-p-benzoquinone.

Remarkably, the anthraquinone-2-carboxylic acid is found to be unsuitable as a modifier when it comes to increasing H_2O_2 electrogeneration. This behavior can be associated with the presence of carboxyl group that deactivates the ring and makes the reduction of the molecule difficult.

The anthraflavic acid (AA) was also seen to less efficient when it comes to the production of H_2O_2. This is probably because of the strong activating hydroxyl groups that enhance the electron density in the ring. Thus, when a molecule is reduced, it is difficult for it to be oxidized again, and this hinders the reduction of O_2 to H_2O_2. The cyclic voltammogram for the material containing anthraflavic acid shows two oxidation peaks and two reduction peaks. These peaks demonstrate that the molecule can undergo a mechanism similar to the one proposed for 2-ethylanthraquinone. In the mechanism proposed for 2-ethylanthraquinone, the molecule undergoes a reduction by 1 electron in a first step and receives a proton, generating a highly reactive radical. The molecule then undergoes a second reduction by another electron and receives another proton; it subsequently reacts with oxygen, generating a superoxide anion that may undergo reduction again or disproportionation to H_2O_2 [14]. However, in the case of anthraflavic acid, the presence of strong activating hydroxyl group makes it more difficult for the molecule to undergo oxidation again and to produce H_2O_2.

The stability of the microporous layers was evaluated by linear sweep voltammetry at 900 rpm. This was repeated after the voltammetries at 100, 400 900, 1600 and 2500 rpm. The currents were found to maintain similar values, indicating stability. A cyclic voltammetry was carried out for the electrolyte saturated with O_2 at scan rate of 50 mV s^{-1} before and after conducting linear sweep voltammetry. No significant differences were also found between the currents, thus indicating stability in these microporous layers (results not shown).

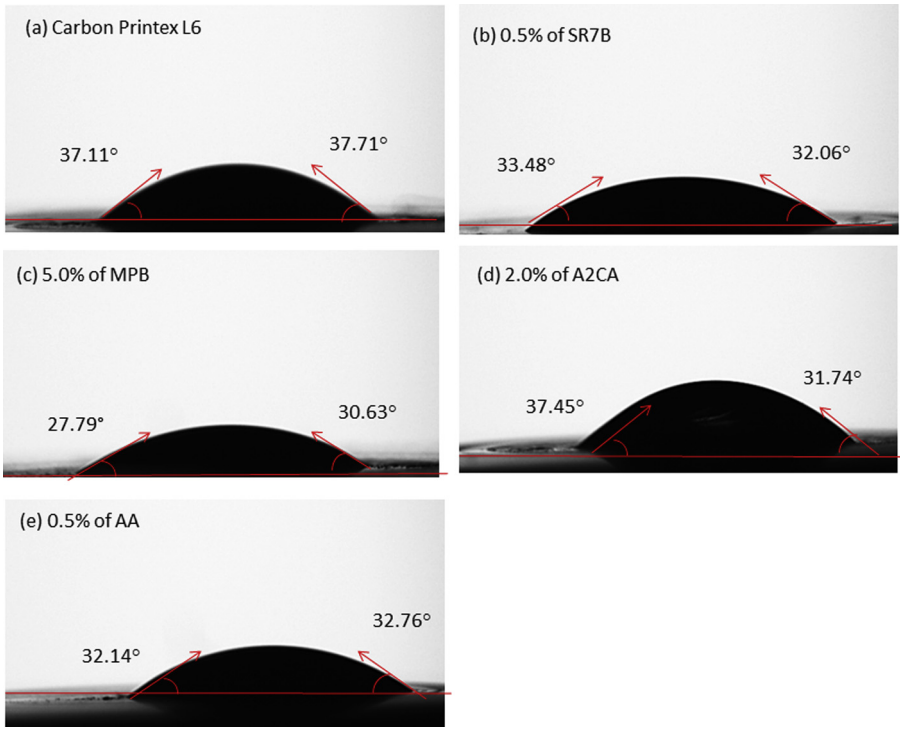

Fig. 3. Photographs of ultrapure water droplets on microporous layers of (a) Carbon Printex L6, (b) 0.5% of Sudan Red 7B, (c) 5.0% of Methyl-p-benzoquinone, (d) 2.0% of Anthraquinone-2-carboxylic acid and (e) 0.5% of Anthraflavic acid.

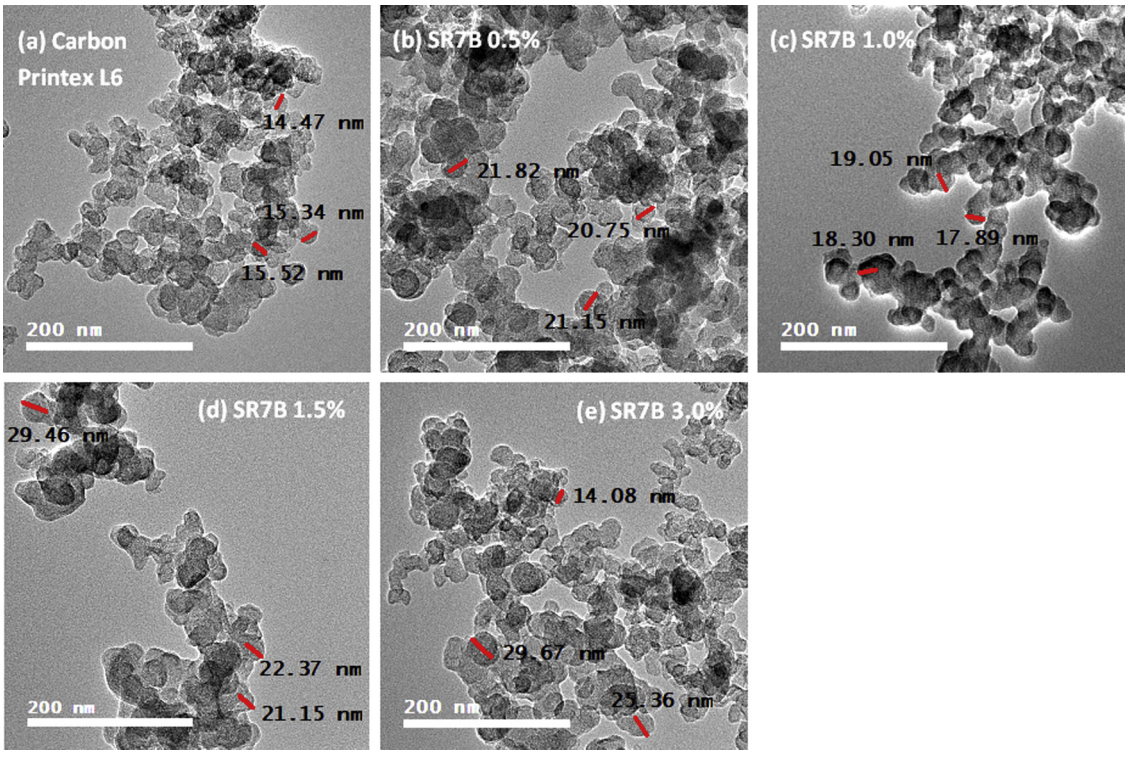

Fig. 4. TEM images with potential sweep at 200,000 V, scale of 200 nm and magnification of 200,000 for (a) Carbon Printex L6, and for materials containing different amounts of Sudan Red 7B - (b) 0.5%, (c) 1.0%, (d) 1.5%, and (e) 3.0%.

3.2. Characterization of electrocatalysts materials

Fig. 3 shows images derived from the calculation of the contact angle with a tension meter for microporous layers composed of carbon Printex L6 and carbon modified with 0.5% of Sudan Red 7B (SR7B), 0.5% of methyl-p-benzoquinone (MPB), 2.0% of anthraquinone-2-carboxylic acid (A2CA) and 0.5% of anthraflavic acid (AA). These proportions of modifiers presented good results relative to the generation of H_2O_2 in RRDE experiments.

As can be observed in Fig. 3, the addition of modifiers contributed to a decrease in the contact angle; this indicates an increase in hydrophilicity of these materials compared to carbon Printex L6. The increase

in hydrophilicity may lead to an increase in H_2O_2 generation. Carbon Printex L6 exhibited a medium contact angle of 37.40°, while materials containing methyl-p-benzoquinone and Sudan Red 7B presented contact angles of 29.21 and 32.77°, respectively. Thus, the materials presented relatively higher hydrophilicity compared to carbon; this is in line with the resultant higher amounts of H_2O_2 produced via the use of RRDE [30,38]. Despite the fact that the material containing 0.5% of anthraflavic acid yielded a contact angle of 32.45°, a value found to be very close to that of Sudan Red 7B, this material was not seen to be much efficient for the production of H_2O_2. Similarly, anthraquinone-2-carboxylic acid was also found to be less efficient for H_2O_2 production in spite of exhibiting a contact angle of 34,59° – a value closer to that of carbon. In short, hydrophilicity is not the only feature that has the ability to influence the production of H_2O_2.

Sudan Red 7B was chosen to be applied on gas diffusion electrodes due to the fact that this modifier yielded a relatively higher current efficiency for hydrogen peroxide electrogeneration in relation to the other materials investigated in this work. In view of that, materials containing different amounts of Sudan Red 7B were analyzed by transmission electron microscopy. This analysis was aimed at verifying whether there were changes in physical characteristics that may be related to higher H_2O_2 electrogeneration. The material containing 5.0% of this modifier did not disperse in isopropyl alcohol and its dispersion in water is found to induce the agglomeration of materials, thus rendering it difficult to carry out TEM analysis. By virtue of that, this proportion was not subjected to investigation.

In Fig. 4(a), the presence of an average particle size of 15 nm for carbon Printex L6 was observed. The small particles exhibited by this type of carbon have the advantage of being characterized by larger exposed (surface) area that enables functional groups to act in oxygen reduction reaction.

The material modified with 0.5% of Sudan Red 7B presented slightly larger particles compared to carbon Printex L6 (shown in Fig. 4b), being around 20 nm, while the material containing 1.0% of this modifier exhibited particles of around 18 nm (shown in Fig. 4c). Materials containing 1.5 and 3.0% of this modifier exhibited particles ranging from 14 nm to 29 nm. Materials containing 0.5 and 1.0% of Sudan Red 7B may have experienced a higher generation of H_2O_2 due to the fact that they maintained their structure more similar to that of carbon Printex L6. The small particles allows the functional groups to be exposed on the surface area so as to act in RRO, facilitating both the arrival of oxygen to active sites (where O_2 is reduced to H_2O_2) and the exit of H_2O_2 [48,49]. Larger proportions of the modifier may be altering the physical characteristics of carbon Printex L6, generating agglomerates, while decreasing the active area of the material and consequently decreasing its efficiency for H_2O_2 generation.

A mechanism was proposed regarding the oxidation and reduction reactions for Sudan Red 7B, since this material has been applied in gas diffusion electrodes. The groups bound to the rings of the molecule were taken into account. The entire Sudan Red 7B molecule is in resonance and the NR_2 group is an activating group of the ring. The N=N (I) group, shown in Fig. 5(a), probably undergoes reduction first, since it has no groups adjacent to it that could prevent the entrance of H^+.

It is known that chemical bonds tend to break if a very high potential is used. This is, however, not the case of the potentials used in this work. The nitrogen that forms part of the NR_2 group can donate electron density to the ring, facilitating the entry of H in the second group N=N (II). The two azo groups may induce the generation of two peaks in cyclic voltammetry since they are in different environments, as can be observed in Fig. 1(d).

Functional groups from the surface of carbon, such as quinones, can effectively play a role in the RRO; this probably applies also to -N = N- groups of Sudan Red 7B that may be reduced and subsequently undergo oxidation as they reduce molecular oxygen generating H_2O_2.

Apart from the oxygen reduction reaction which occurs on the surface of carbon that is polarized by electrochemical mechanism as shown in Fig. 5(b) (A), the process may likewise occur by chemical mechanism. In this chemical mechanism, the modifying molecule undergoes reduction as a result of the polarization on the electrode. The modifying molecule subsequently undergoes oxidation when it reduces O_2 to H_2O_2. The molecule is then rapidly reduced again by polarization on the electrode, thus acting as a catalyst for the RRO as outlined in Fig. 5(b) (B). This mechanism could be compared to the anthraquinone autooxidation commercial process used for hydrogen peroxide production in which 2-alkylanthraquinone (AQ), generally 2-ethyl or 2-tert-butyl, in organic medium is hydrogenated by $H_{2(g)}$ in the presence of a catalyst such as palladium, producing the 2-alkylanthrahydroquinone (AHQ). Then, AHQ is separated from the catalyst, and oxidized by $O_{2(g)}$, regenerating the AQ and producing hydrogen peroxide. The hydrogen peroxide produced is extracted into as aqueous medium and concentrated [50,51].

The Sudan red 7B modifier acts as AQ, since its reduction and subsequent oxidation also lead producing H_2O_2. In the commercial process the reduction of the anthraquinone is carried out in organic medium while in this work the reduction of Sudan Red 7B is done by the polarization of the electrode. Therefore, the mechanism is called chemical / electrochemical. One of the advantages of this chemical / electrochemical process for H_2O_2 generation in relation to the commercial process is the non-use of organic reagents and hydrogen gaseous with high pressure which requires care in both transport and storage.

3.3. Electrogeneration of H_2O_2 on modified GDE with 0.5% of Sudan Red 7B

Gas diffusion electrodes of unmodified carbon and carbon Printex L6 modified with 0.5% of Sudan Red 7B were developed by sintering at 220 °C. This was carried out owing to the loss of mass of the modifier at 220 °C which was observed through thermogravimetric analyses (TGA) of Sudan Red 7B (results not shown).

The results obtained after conducting electrolysis are shown in Fig. 6. It was observed that the occurrence of stabilization in H_2O_2 concentration after 60 min of electrolysis. This can be attributed to the equilibrium established between the cathode reaction involving the formation of H_2O_2 on the working electrode and the reactions involving the degradation of H_2O_2. The degradation of H_2O_2 may occur by reaction on the cathode, where H_2O_2 undergoes a second reduction via 2 electrons, generating water. The degradation may also occur on the anode, where H_2O_2 can undergo oxidation. H_2O_2 may also either undergo chemical decomposition in solution or react with the products of oxygen reduction reaction on the cathode. These reactions are shown in the equations below [52]:

$$\text{Reduction on the cathode } H_2O_2 + 2H^+ + 2e^- \rightarrow 2H_2O \quad (3)$$

$$\text{Oxidation on the anode } H_2O_2 \rightarrow O_2 + 2H^+ + 2e^- \quad (4)$$

$$\text{Chemical decomposition in solution } 2H_2O_2 \rightarrow O_2 + 2H_2O \quad (5)$$

$$O_2^- + H_2O_2 \rightarrow OH^- + O_2 + {}^{\cdot}OH^* \quad (6)$$

$${}^{\cdot}HO_2 + H_2O_2 \rightarrow O_2 + H_2O + {}^{\cdot}OH^* \quad (7)$$

$${}^{\cdot}OH + H_2O_2 \rightarrow {}^{\cdot}HO_2 + H_2O^* \quad (8)$$

*(6)–(8) are reactions with products of oxygen reduction reaction on the cathode.

The highest concentrations of H_2O_2 produced for carbon Printex L6 GDE and GDE modified with 0.5% of Sudan Red 7B were 770.7 mg L^{-1} and 1025.9 mg L^{-1}, respectively, both at 100 mA cm^{-2}. The graph in Fig. 7 compares concentrations at the end of each electrolysis (after 90 min) for both modified and unmodified GDE as a function of applied current. Based on the illustrated results, it was observed that at 75, 100 and 150 mA cm^{-2}, the modified GDE generated more H_2O_2 than the unmodified one; this is probably because at these current densities the

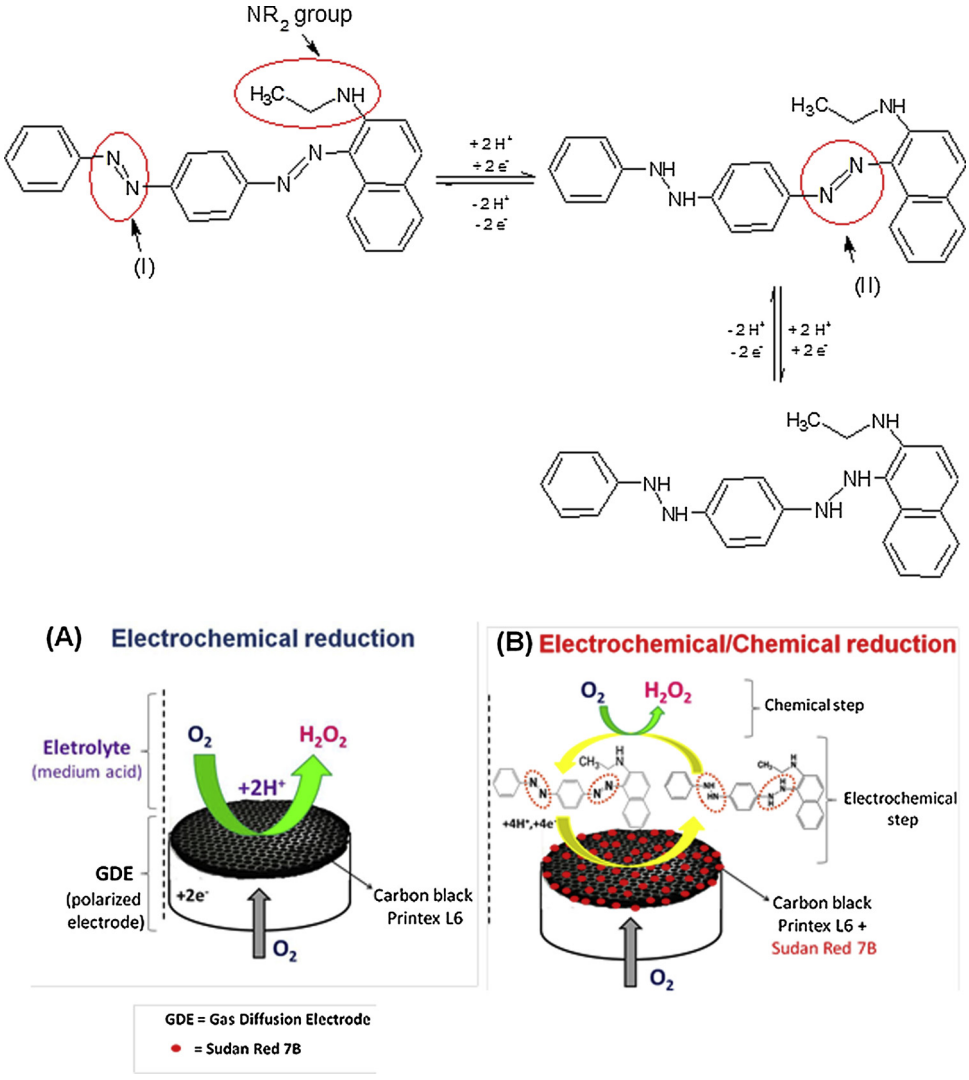

Fig. 5. (a) Proposed mechanism for oxidation and reduction reactions in Sudan Red 7B molecule. (b) (A) Proposed mechanism for electrochemical reduction of oxygen. (b) (B) Proposed mechanism for electrochemical/chemical reduction of oxygen.

modifier can act as a catalyst of the reaction, participating in both the chemical and electrochemical mechanisms for H_2O_2 generation. The electrochemical mechanism occurs on the surface of the electrode with direct reduction of oxygen, and the electrochemical/chemical mechanism involves the electrochemical reduction of the modifier followed by the chemical mechanism in which the modifier is oxidized while the oxygen is reduced to H_2O_2.

Remarkably, no significant increase was observed in the concentration of H_2O_2 generated when the current density was increased from 75 to 100 mA cm^{-2} for both the modified and unmodified electrodes. The application of current density of 150 mA cm^{-2} led to a decrease in H_2O_2 generation for both electrodes. This behavior can be attributed to the fact that there is an increase in charge at the triple interface of the GDE formed by gas/electrolyte/electrode that can favor the generation of water via reduction of H_2O_2 by 2 electrons, or via reduction of oxygen via 4 electrons.

The studies conducted on kinetic rate constant, energy consumption and current efficiency show which of the current densities for each electrode could be more advantageous for application in advanced oxidation processes.

The graphs related to hydrogen peroxide generation as a function of time in Fig. 6 show that the generation of H_2O_2 is almost linear in relation to time in the first 20 min of electrolysis. It is worth noting that the generation of H_2O_2 depends on the adsorption of oxygen on the surface of the electrode, and this in turn occurs in two stages with different rate constants. A rate constant related to H_2O_2 generation from the oxygen adsorbed on the surface of the electrode and another rate constant for the desorption of H_2O_2 from the surface of the electrode into solution, apart from other parallel reactions such as water generation from oxygen, H_2O_2 reduction to water, and oxidation of H_2O_2 on the anode [45].

For the GDE, the oxygen reduction reactions occur at the triple interface formed by gas/electrolyte/electrode, and oxygen is supplied directly and constantly at the interface, which is pressurized at the outer face of the electrode. In this sense, oxygen ceases to be a limiting reactant of reaction, and as such, ORR does not depend on oxygen dissolved in the solution. As the medium is acidic, the reactions in this case would also not be dependent upon the concentration of H^+ ions. Thus, the reaction constant can be said to be controlled by apparent kinetic constant of zero pseudo-order; in other words, the generation of H_2O_2 will be independent of both the concentration of O_2 molecules and the H^+ ions present in excess at the interface [14,23,26,27,46].

Therefore, a linear regression can be applied to the collinear points of the first 20 min of the graphs of Fig. 6, and thus determine the angular coefficients representing the apparent kinetic constants (k_{ap}) for each current density according to the following equation where C_t is the concentration of H_2O_2 at time t:

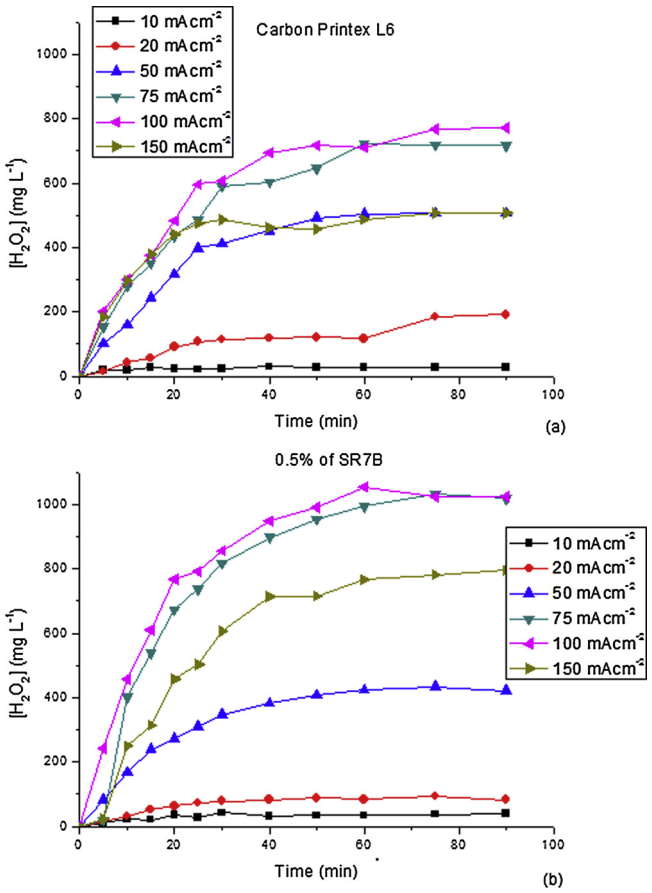

Fig. 6. Hydrogen peroxide concentration produced as a function of time for carbon Printex L6 GDE in (a) and for GDE with 0.5% of Sudan Red 7B in (b) for 90 min of electrolysis at constant current using 0.1 mol L^{-1} of K_2SO_4 as electrolyte at pH 3 and acidified with H_2SO_4.

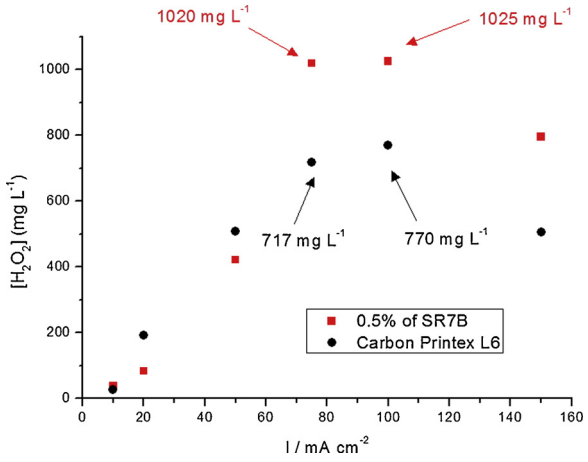

Fig. 7. Final concentrations of hydrogen peroxide after 90 min of electrolysis as a function of applied current for carbon Printex L6 GDE and GDE modified with 0.5% of Sudan Red 7B. The following conditions were applied here: O_2 pressure of 0.3 bar, using 0.1 mol L^{-1} of K_2SO_4 as electrolyte at pH 3 and acidified with H_2SO_4.

$$Ct = -kap.\ t$$

Fig. 8 shows the graph that compares the different apparent kinetic constants obtained for each experiment for both types of electrodes. At current densities of 10, 20 and 50 mA cm^{-2}, the rate constants are found to be very similar for the two types of GDE. At current densities of

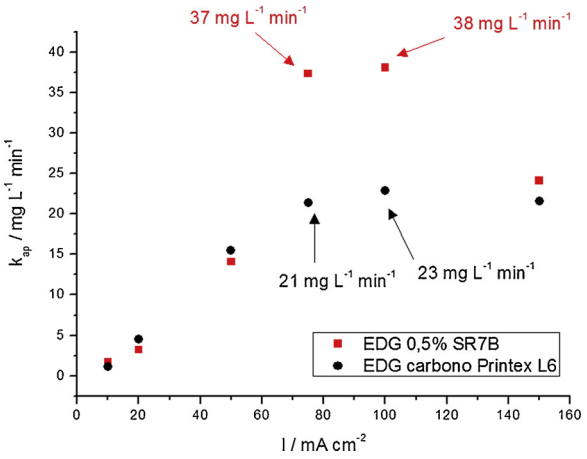

Fig. 8. Apparent kinetic constants (k_{ap}) for reactions related to the formation of hydrogen peroxide as a function of applied current density. These results are based on the first 20 min of reaction for the carbon Printex L6 GDE and the GDE modified with 0.5% of Sudan Red 7B.

20 and 50 mA cm^{-2}, the rate constants are slightly higher for the carbon Printex L6 GDE. At the current density of 10 mA cm^{-2}, the values are also found to be very similar. For current densities of 75 and 100 mA cm^{-2}, the constants are seen to be relatively higher for the modified GDE while at 150 mA cm^{-2} the difference between the constants becomes smaller again, though still higher for the modified electrode.

The differences observed in apparent kinetic constants probably stem from the presence of the organic modifier in the carbon Printex L6 matrix. These kinetic constants are related to the reactions from the adsorption of oxygen to the desorption of H_2O_2 into solution. In this context, the quantity of the modifier may have improved the efficiency of the generation of H_2O_2 in an efficient and selective fashion for H_2O_2 generation, thereby increasing the apparent kinetic constants. Furthermore, the electrochemical/chemical mechanism stemming from the presence of the modifier may favor the production of H_2O_2 and the modifier may be acting by reducing the parallel reactions such as the reduction of H_2O_2 to water or the reduction of oxygen to water.

Apart from the apparent kinetic constant, another important parameter to be evaluated is the energy consumption. This parameter plays a relevant economic role in the sense that it is related to the costs incurred during the reaction process and can be calculated according to the equation [53]:

$$E.\ C. = \frac{i.\ E.\ t}{m}$$

where, *E.C.* is the energy consumption in kWh kg^{-1}, *i* is the current in A, *E* is the cell potential in V, t is the time in hours and m being the mass of H_2O_2 electrogenerated in kg. The results obtained are shown in Fig. 9.

The graphs that correlate the energy consumption as a function of the current densities applied relative to the carbon Printex L6 GDE show a tendency of an increase in consumption with a corresponding increase in the applied current density from 20 mA cm^{-2} to 50, 75, 100 and 150 mA cm^{-2}. This is, however, not observed at 10 mA cm^{-2} where the consumption is greater than at 20 mA cm^{-2}. This may attribute to the low H_2O_2 production at this current density. At 150 mA cm^{-2}, a decrease is observed in H_2O_2 generation while the energy consumption increases, reaching its highest value.

Taking these results into account, the best current densities for the carbon Printex L6 GDE are 20, 50, 75 and 100 mA cm^{-2}. At these densities, the concentrations obtained at the end of 90 min of electrolysis were 191.4, 507.4; 717.3 and 770.7 mg L^{-1}, while the energy consumed was 70.1, 120.6, 168.5 and 247.0 kW h kg^{-1}, respectively. A

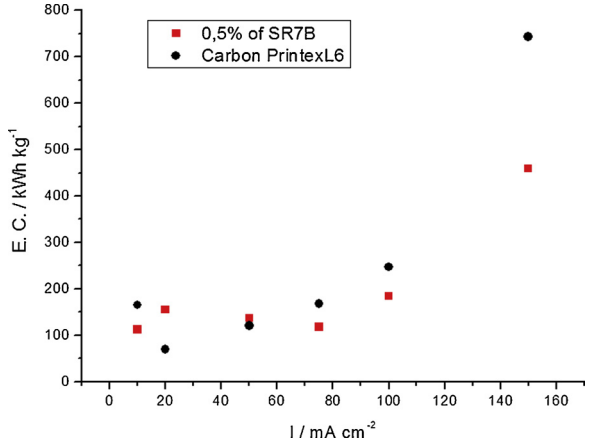

Fig. 9. Energy consumption as a function of the current density applied during the electrolysis on carbon Printex L6 GDE and on GDE modified with 0.5% of Sudan Red 7B.

further observation that deserves mentioning is that the current density of 20 or 50 mA cm^{-2} may be used for AOP application, since an amount between 100–500 mg L^{-1} of H_2O_2 is generally used in the degradation of pollutant molecules [46,53–56].

For the GDE modified with 0.5% of Sudan Red 7B, a relatively lower generation of H_2O_2 was observed at 10 and 20 mA cm^{-2}, with the results obtained being 39.1 and 82.9 mg L^{-1} respectively. An increase in energy consumption from 112.3 to 154.4 kW h kg^{-1} was also observed when the current was increased from 10 to 20 mA cm^{-2}, respectively. At both current densities of 50 and 75 mA cm^{-2}, there was an increase in the generation of H_2O_2 and a decline in energy consumption. From 75 to 100 mA cm^{-2}, no significant increase was observed in the H_2O_2 concentration produced, yet an increase was observed in energy consumption, probably due to the higher energy consumption required for the application of the highest current density (100 mA cm^{-2}). In view of that, the best current densities chosen for the modified electrode were 50, 75 and 100 mA cm^{-2}; these current densities led to the generation of 421.9, 1020.1 and 1025.9 mg L^{-1} of H_2O_2 and energy consumption of 136.6, 118.0 and 184.5 kW h kg^{-1}, respectively. Finally, at 150 mA cm^{-2}, the H_2O_2 generation decreased to 795.2 mg L^{-1}, leading to an increase in energy consumption to 459.5 kW h kg^{-1}.

For OAP application, the modified electrode is found to be better in cases where the goal is to generate higher amounts of H_2O_2. This is because at 50 mA cm^{-2}, the unmodified electrode is advantageous when it comes to energy consumption. For the fact that no significant increase in H_2O_2 generation is observed when the energy consumption in the modified GDE increases from 75 to 100 mA cm^{-2}, the current density of 75 mA cm^{-2} is remarkably better. When the current densities of 75 and 100 mA cm^{-2} for the modified and unmodified GDEs is compared, the modified electrode is seen to be more advantageous, in that it is characterized by a relatively lower energy consumption and higher generation of H_2O_2. In short, the carbon modified GDE requires an energy consumption of 118.0 kW h kg^{-1} to generate 1020.1 mg L^{-1} of H_2O_2, while the unmodified GDE requires an energy consumption of 168.5 kW h kg^{-1} to produce 717.3 mg L^{-1} of H_2O_2 at the current density of 75 mA cm^{-2} for both electrodes. This makes the modified GDE more advantageous compared to the unmodified.

When the GDE modified with Sudan Red 7B and the GDE modified with other organic molecules are compared, it is observed that the former in this experimental configuration turned out to be the best in terms of H_2O_2 generation. This can be explained by the fact that the GDE modified with Sudan Red 7B was capable of producing up to 1020 mg L^{-1} of H_2O_2, whereas the unmodified GDE produced 717 mg L^{-1} of H_2O_2. The GDE modified with 5.0% of cobalt (II) phthalocyanine produced 331 mg L^{-1} of H_2O_2 [22] and the GDE modified with 5% of iron (II) phthalocyanine led to the generation of 240 mg L^{-1} of H_2O_2 [25]; these results differ from the results obtained for the unmodified carbon Printex L6 GDE which produced around 176 mg L^{-1} of H_2O_2. GDE modified with 1.0% of tert-butyl anthraquinone produced 301 mg L^{-1} of H_2O_2, whereas the carbon Printex L6 GDE produced 182 mg L^{-1} of H_2O_2 [23]. The use of GDE with 10% of 2-ethylanthraquinone, azobenzene and 2-tert-butylanthraquinone resulted in an increase in hydrogen peroxide generation reaching 700 mg L^{-1} for the first two molecules and 850 mg L^{-1} for the latter molecule, while only 100 mg L^{-1} of H_2O_2 was obtained for the carbon Printex L6 GDE [24,45]. The GDE modified with 10% of azobenzene led to the production of almost 700 mg L^{-1} of H_2O_2 [27]. With regard to energy consumption, the GDE modified with 5% of iron (II) phthalocyanine led to an energy consumption of 165 kW h Kg^{-1}, while the unmodified carbon Printex L6 GDE led to the consumption of 300 kW h Kg^{-1} in acid medium [25]. Furthermore, the use of 2-ethylanthraquinone, azobenzene and 2-tert-butylanthraquinone led to a reduction of energy consumption from around 596 to 232 kW h kg^{-1} [24,45]. The GDE modified with Sudan Red 7B in this study led to an energy consumption of 118.0 kW h kg^{-1}, while the unmodified GDE consumed around 168.5 kW h kg^{-1} of energy.

In Fig. 9, it can observe that at 10 mA cm^{-2} the modified GDE has a lower energy consumption compared to the unmodified. This comes as no surprise because the modifier leads to higher H_2O_2 generation. Nonetheless, at 20 mA cm^{-2} the unmodified GDE exhibits lower energy consumption compared to the modified GDE; this is because the energy consumption also depends on the cell potential, and this may have been a much greater influential factor than the higher H_2O_2 generation, making the result different from what was expected.

At 50 mA cm^{-2}, the energy consumption values are found to be very similar for both the modified and unmodified electrodes, while at 75, 100 and 150 mA cm^{-2} the energy consumption is seen to be higher for the carbon Printex L6 electrode. Lower energy consumption was observed for the electrode modified with 0.5% of Sudan Red 7B. This is probably due to the effect of the modifier on the reactions. The modifier in this case adds an electrochemical/chemical mechanism to the process, acting as a catalyst and promoting a higher production of H_2O_2.

Higher current densities, such as 150 mA cm^{-2}, lead to higher energy consumption yet lower H_2O_2 generation. This is probably due to the increase in the current employed for parallel reactions, such as the hydrogen evolution reaction.

The addition of the organic modifier may have led to a selectivity of ORR for H_2O_2 generation. It may have also altered the reaction kinetic constant, which was increased in the current densities of 75, 100 and 150 mA cm^{-2}, leading to lower energy consumption in the production of H_2O_2.

It is worth pointing out that based on the results obtained from the linear voltammograms in RRDE, the aforementioned outcomes came as a surprise, since there was no change in the ORR starting potential. However, the increase observed in both the hydrogen peroxide generation and the apparent kinetic constant was seen as sufficient to promote lower energy consumption.

Current efficiency (C.E.) was also calculated for each electrolysis for both the modified and unmodified electrodes according to the equation below:

$$C.\,E. = \left(\frac{mH_2O_2 obtained}{mH_2O_2 theoretical}\right) \times 100 = \left(\frac{mH_2O_2 obtained}{i{*}t{*}34/2F}\right) \times 100$$

Where $m\,H_2O_2\,obtained$ represents the mass of H_2O_2 obtained after 90 min of electrolysis in g, i is the current applied in A, t is the time of electrolysis in seconds, 2 is related to the stoichiometric number of transferred electrons and F is the Faraday constant (96,486 C mol^{-1}). The following equation was also considered for the ORR:

$$O_2 + 2H^+ + 2e^- \rightarrow H_2O_2 \quad (3)$$

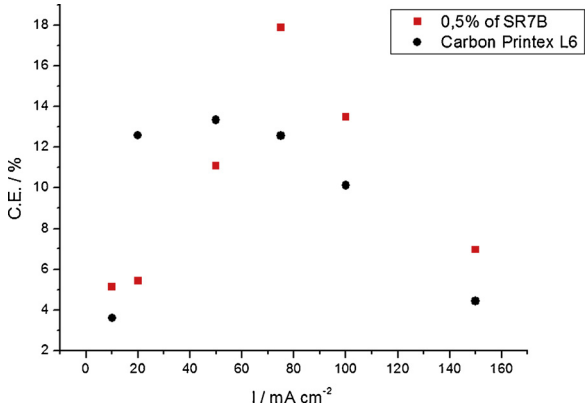

Fig. 10. Current efficiency as a function of the current density applied during electrolysis using carbon Printex L6 GDE and GDE modified with 0.5% of Sudan Red 7B.

The current efficiency provides information regarding the quantity of current used for the generation of H_2O_2 or for the generation of other molecules, such as water or hydrogen.

Fig. 10 shows the current efficiency of each current density for both electrodes. The curve for carbon Printex L6 GDE shows an increase in current efficiency as the current density is increased until 50 mA cm^{-2}. From this current density onwards up to 150 mA cm^{-2} it is possible observe that an increase in current density leads to a decrease in current efficiency. This is probably because the current may be promoting the production of other molecules instead of H_2O_2. In this sense, the best current densities are 50 and 75 mA cm^{-2}. At these current densities, the concentrations obtained at the end of 90 min of electrolysis were 507.4 and 717.3, with energy consumption of 120.6 and 168.5, and current efficiency of 13.3 and 12.6%, respectively.

For the modified GDE, an increase in current efficiency is observed given an increase in the current density applied. This observation is valid until 75 mA cm^{-2}. From this current density onwards up to 150 mA cm^{-2} the current efficiency decreases. Thus, the best current densities chosen for the modified electrode were 75 and 100 mA cm^{-2}. These current densities yield 1020.1 and 1025.9 mg L^{-1} of H_2O_2, energy consumption of 118.0 and 184.5 kW h kg^{-1}, and current efficiency of 17.9 and 13.5%, respectively.

When the modified and unmodified GDEs are compared with respect to current efficiency, the former is found to be more advantageous at the current densities of 10, 75 and 100 mA cm^{-2}. This advantage comes as no surprise because the modifier leads to higher H_2O_2 generation probably as a result of the catalytic effect it exerts on the reactions by adding an electrochemical/chemical mechanism to the process. However, at the current densities of 20 and 50 mA cm^{-2}, the unmodified GDE exhibits higher current efficiency than the modified; this is probably because carbon Printex L6 leads to H_2O_2 generation rather than inducing other reactions. At the current densities of 50, 75 and 100 mA cm^{-2}, the modified GDE yields an increase in current efficiency of 42, 33 and 57%, respectively, in comparison to the unmodified GDE. At the current density of 75 mA cm^{-2}, the modified GDE is found to promote a greater production of H_2O_2, with relatively higher apparent kinetic constant and current efficiency yet with lower energy consumption compared to the unmodified GDE. This makes the modified GDE suitable as a candidate for application in OAP.

Thus, the application of gas diffusion electrodes with carbon Printex L6 modified with 0.5% of Sudan red 7B can lead to a higher generation of H_2O_2, with a higher apparent kinetic constant yet with a relatively lower energy consumption compared to the unmodified GDE. Indeed, these properties make the modified electrode advantageous for applications in advanced oxidative processes. The modified electrode was also able to generate higher concentrations of H_2O_2 that can be applied in systems that may require high concentrations of this reagent compared to the amount of H_2O_2 generated using the unmodified GDE.

Electrolysis was carried out for 4 h to evaluate the stability of the GDEs under investigation. The current densities of 50 mA cm^{-2} and 75 mA cm^{-2} were applied for the carbon Printex L6 GDE and the GDE modified with 0.5% of Sudan Red 7B, respectively (Fig. S1 at the supplementary information). This is because the best results were obtained at these current densities with regard to energy consumption, apparent kinetic constants, concentration of H_2O_2 electrogenerated, current efficiency and possibility of application in AOP. For the carbon Printex L6 GDE, it was observed an increase in the concentration curve up to about 60 min, Fig. S1a. From this period onwards, the concentration curve stays constant and a slight decay is noted from 175 min onwards up to the end of the 240 min of reaction.

The aforementioned constant region (between 60 and 125 min) may stem from the equilibrium between the formation of H_2O_2 on the cathode and its degradation on the anode or may be induced by the reduction via 2 electrons leading to water generation on the cathode among other parallel reactions that may occur in the electrolyte [52]. The decay observed here can be attributed to the fact that the H_2O_2 concentration may have become so high to the point where it undergoes reduction rather than the oxygen itself on the cathode. In this context, the application of this system toward the degradation of molecules can favor the generation of H_2O_2, since H_2O_2 may be consumed in the process of degradation of the organic molecules, displacing the reaction to generate more H_2O_2.

The results obtained for the GDE modified with 0.5% of Sudan Red 7B demonstrate, once again, that after 60 min of reaction the concentration of H_2O_2 generated becomes almost constant, Fig. S1b. This is attributed to the balance between the generation and degradation of H_2O_2. Interestingly, no decay was, however, observed in H_2O_2 concentration probably because the presence of the modifier tends to promote a greater selectivity for oxygen reduction, even if the H_2O_2 concentration is high in the solution.

Another study has made to verify the stability of the catalyst material was the evaluation of the voltammetric profile of EDG before each experiment. Linear voltammetries were performed in electrolyte saturated with $O_{2(g)}$ and it was verified that the voltammetric profile of EDG remained constant even after several experiments, which proves the stability of the material, Fig. S2.

The repeatability study for the GDE modified with 0.5% of Sudan Red 7B was conducted by electrolysis in triplicate for 90 min on the same electrode at a current density of 50 mA cm^{-2} and with three electrodes made on different days, Fig. S3 at the supplementary information. At the end of the three electrolysis processes conducted on a single electrode, a mean H_2O_2 concentration of 458.5 ± 8.0 mg L^{-1} was obtained. The electrodes produced on different days exhibited a mean H_2O_2 concentration of 429.6 ± 17.3 mg L^{-1}. The standard deviation value was found to be less than 5% of the mean of the concentrations. This indicates a significant degree of accuracy of the experiments with agreement between the results.

Table 2 shows a summary of the concentrations of hydrogen peroxide produced at the end of 90 min of each electrolysis, the apparent kinetic constant, the energy consumption and current efficiency at current densities of 10, 20, 50, 75, 100 and 150 mA cm^{-2} for the carbon Printex L6 GDE and the GDE modified with 0.5% of Sudan Red 7B.

The carbon Printex L6 GDE at the current density of 50 mA cm^{-2} presented the best results considering the studied parameters. For the modified GDE with 0.5% of Sudan Red 7B, the best results were obtained at the current density of 75 mA cm^{-2}. In view of that, it can conclude that the modified GDE is a good option to use in systems that need high H_2O_2 concentrations.

4. Conclusion

Experiments with rotating ring-disc electrodes (RRDE) showed that

Table 2
Summary of the concentrations of H_2O_2 produced at the end of 90 min of electrolysis ($[H_2O_2]_f$), the apparent kinetic constant (k_{ap}), the energy consumption (E.C.) and current efficiency (C.E.) at different current densities (I) for the carbon Printex L6 GDE (CP) and GDE modified with 0.5% of Sudan Red 7B (0,5% SR7B).

I (mA cm^{-2})	$[H_2O_2]_f$ (mg L^{-1}) CP	($[H_2O_2]_f$) (mg L^{-1}) 0.5% SR7B	k_{ap} (mg L^{-1} min^{-1}) CP	k_{ap} (mg L^{-1} min^{-1}) 0.5% SR7B	E.C. (kWh kg^{-1}) CP	E.C. (kWh kg^{-1}) 0.5% SR7B	C.E. (%) CP	C.E. (%) 0.5% SR7B
10	27.3	39.1	1.1	1.6	165.0	112.3	3.6	5.1
20	191.4	82.9	4.5	3.2	70.1	154.4	12.6	5.4
50	507.4	421.9	15.5	14.1	120.6	136.6	13.3	11.1
75	717.3	1020.1	21.4	37.3	168.5	118.0	12.6	17.9
100	770.7	1025.9	22.9	38.1	246.9	184.5	10.1	13.5
150	506.4	795.2	21.5	24.1	743.5	459.5	4,4	6.9

catalytic materials with 5.0% of MPB, 2.0% of A2CA, 0.5% of AA and 0.5% of SR7B presented great current efficiency in the electrogeneration of hydrogen peroxide. The use of materials containing modifiers contributed toward a higher generation of hydrogen peroxide compared to the use of carbon Printex L6 materials without modifiers. Based on the results obtained from the RRDE, the material containing 0.5% of SR7B was chosen for the production of gas diffusion electrodes aiming at studying the activity of this modifier in the electrogeneration of H_2O_2.

The application of current density of 75 mA cm^{-2} for the electrode modified with acid electrolyte led to the generation of 1020.1 mg L^{-1} of H_2O_2 with energy consumption of 118.0 kW h kg^{-1}, apparent kinetic constant of 37.3 mg L^{-1} min^{-1} and current efficiency of 17.9%. By contrast, the unmodified electrode generated 717.3 mg L^{-1} of H_2O_2 with energy consumption of 168.5 kW h kg^{-1}, apparent kinetic constant of 21.4 mg L^{-1} min^{-1} and current efficiency of 12.6% at the same current density. The current efficiency was increased by 42% for the modified GDE in comparison to the unmodified GDE.

In terms of H_2O_2 electrogeneration, the modified GDE produced better results as expected from the results derived from the application of the RRDE. In addition, the modified GDE also yielded higher apparent kinetic constant values and lower energy consumption. The lower energy consumption observed for the modified GDE seemed to be in disagreement with the results obtained from the RRDE that showed no shift in the RRO starting potential in linear sweep voltammograms, which is indicative of lower energy consumption. The electrochemical/chemical mechanism, which yields a higher generation of H_2O_2 along with its selectivity for H_2O_2 electrogeneration, may have been responsible for these results.

The results of our investigation show that carbon Printex L6 gas diffusion electrodes modified with 0.5% SR7B can be applied in advanced oxidative processes requiring high hydrogen peroxide concentrations of approximately 1000 mg L^{-1} in acidic medium and under the conditions applied in this work.

Acknowledgements

The authors acknowledge the financial support provided by the Brazilian funding agencies including the Brazilian National Council for Scientific and Technological Development - CNPq (grants no. 465571/2014-0, 301492/2013-1, 302874//2017-8 and 427452/2018-0), São Paulo Research Foundation (FAPESP – grants #2011/14314-1, #2014/50945-4, #2016/01937-4, #2016/08760-2 and #2017/10118-0) and the Coordenação de Aperfeiçoamento de Pessoal de Nível Superior – Brasil (CAPES) – Finance Code 001.

Appendix A. Supplementary data

Supplementary material related to this article can be found, in the online version, at doi:https://doi.org/10.1016/j.apcatb.2019.01.071.

References

[1] Ma. Oturan, J.-J. Aaron, Advanced oxidation processes in water/wastewater treatment: principles and applications. A review, Crit. Rev. Environ. Sci. Technol. (2014) 140225124605005, , https://doi.org/10.1080/10643389.2013.829765.
[2] F.C. Moreira, R.A.R. Boaventura, E. Brillas, V.J.P. Vilar, Electrochemical advanced oxidation processes: a review on their application to synthetic and real wastewaters, Appl. Catal. B Environ. 202 (2017) 217–261, https://doi.org/10.1016/j.apcatb.2016.08.037.
[3] G. Boczkaj, A. Fernandes, Wastewater treatment by means of advanced oxidation processes at basic pH conditions: a review, Chem. Eng. J. 320 (2017) 608–633, https://doi.org/10.1016/j.cej.2017.03.084.
[4] L. Feng, E.D. van Hullebusch, M.A. Rodrigo, G. Esposito, M.A. Oturan, Removal of residual anti-inflammatory and analgesic pharmaceuticals from aqueous systems by electrochemical advanced oxidation processes. A review, Chem. Eng. J. 228 (2013) 944–964, https://doi.org/10.1016/j.cej.2013.05.061.
[5] C.C.I. Guaratini, V.B. Zanoni, Corantes Têxteis, Quim. Nova 23 (2000) 71–78.
[6] Y. Luo, W. Guo, H.H. Ngo, L.D. Nghiem, F.I. Hai, J. Zhang, S. Liang, X.C. Wang, A review on the occurrence of micropollutants in the aquatic environment and their fate and removal during wastewater treatment, Sci. Total Environ. 473–474 (2014) 619–641, https://doi.org/10.1016/j.scitotenv.2013.12.065.
[7] D.P. Mohapatra, S.K. Brar, R.D. Tyagi, P. Picard, R.Y. Surampalli, Analysis and advanced oxidation treatment of a persistent pharmaceutical compound in wastewater and wastewater sludge-carbamazepine, Sci. Total Environ. 470–471 (2014) 58–75, https://doi.org/10.1016/j.scitotenv.2013.09.034.
[8] M.L. Wilde, S. Montipó, A.F. Martins, Degradation of β-blockers in hospital wastewater by means of ozonation and Fe2+/ozonation, Water Res. 48 (2014) 280–295, https://doi.org/10.1016/j.watres.2013.09.039.
[9] L. Inácio, E. Ibge, D.W. Tai, Pesquisa Nacional de Saneamento Básico, (2008).
[10] M. Klavarioti, D. Mantzavinos, D. Kassinos, Removal of residual pharmaceuticals from aqueous systems by advanced oxidation processes, Environ. Int. 35 (2009) 402–417, https://doi.org/10.1016/j.envint.2008.07.009.
[11] O. Ganzenko, D. Huguenot, E.D. van Hullebusch, G. Esposito, M.A. Oturan, Electrochemical advanced oxidation and biological processes for wastewater treatment: a review of the combined approaches, Environ. Sci. Pollut. Res. 21 (2014) 8493–8524, https://doi.org/10.1007/s11356-014-2770-6.
[12] M.A. Oturan, E. Brillas, Electrochemical advanced oxidation processes (EAOPs) for environmental applications, Port. Electrochim. Acta 25 (2007) 1–18, https://doi.org/10.4152/pea.200701001.
[13] Z. Qiang, J. Chang, C. Huang, Electrochemical generation of hydrogen peroxide from dissolved oxygen in acidic solutions, Water Res. 36 (2002) 85–94, https://doi.org/10.1016/S0043-1354(01)00235-4.
[14] J.C. Forti, R.S. Rocha, M.R.V. Lanza, R. Bertazzoli, Electrochemical synthesis of hydrogen peroxide on oxygen-fed graphite/PTFE electrodes modified by 2-ethylanthraquinone, J. Electroanal. Chem. 601 (2007) 63–67, https://doi.org/10.1016/j.jelechem.2006.10.023.
[15] T. Salvador, L.H. Marcolino, DEGRADAÇÃO DE CORANTES TÊXTEIS E REMEDIAÇÃO DE RESÍDUOS DE TINGIMENTO POR PROCESSOS FENTON, FOTO-FENTON E ELETRO-FENTON, Quim. Nova 35 (2012) 932–938.
[16] O. Legrini, E. Oliveros, A.M. Braun, Photochemical processes for water treatment, Chem. Rev. 93 (1993) 671–698, https://doi.org/10.1021/cr00018a003.
[17] E.A. Ticianelli, G.A. Camara, Luis G.R.A. Santos, ELETROCATÁLISE DAS REAÇÕES DE OXIDAÇÃO DE HIDROGÊNIO E DE REDUÇÃO DE OXIGÊNIO, Quim. Nova 28 (2005) 664–669.
[18] T. Liu, K. Wang, S. Song, A. Brouzgou, P. Tsiakaras, Y. Wang, New electro-fenton gas diffusion cathode based on nitrogen-doped graphene@carbon nanotube composite materials, Electrochim. Acta 194 (2016) 228–238, https://doi.org/10.1016/j.electacta.2015.12.185.
[19] Y. Wang, Y. Liu, K. Wang, S. Song, P. Tsiakaras, H. Liu, Preparation and characterization of a novel KOH activated graphite felt cathode for the electro-Fenton process, Appl. Catal. B Environ. 165 (2015) 360–368, https://doi.org/10.1016/j.apcatb.2014.09.074.
[20] Z. Pan, K. Wang, Y. Wang, P. Tsiakaras, S. Song, In-situ electrosynthesis of hydrogen peroxide and wastewater treatment application: a novel strategy for graphite felt activation, Appl. Catal. B Environ. 237 (2018) 392–400, https://doi.org/10.1016/j.apcatb.2018.05.079.
[21] E. Yeager, Electrocatalysts for O2 reduction, Electrochim. Acta 29 (1984) 1527–1537, https://doi.org/10.1016/0013-4686(84)85006-9.
[22] W.R.P. Barros, R.M. Reis, R.S. Rocha, M.R.V. Lanza, Electrogeneration of hydrogen peroxide in acidic medium using gas diffusion electrodes modified with cobalt (II) phthalocyanine, Electrochim. Acta 104 (2013) 12–18, https://doi.org/10.1016/j.electacta.2013.04.079.
[23] R.B. Valim, R.M. Reis, P.S. Castro, A.S. Lima, R.S. Rocha, M. Bertotti, M.R.V. Lanza, Electrogeneration of hydrogen peroxide in gas diffusion electrodes modified with tert-butyl-anthraquinone on carbon black support, Carbon N. Y. 61 (2013) 236–244, https://doi.org/10.1016/j.carbon.2013.04.100.
[24] J.C. Forti, M.R.V. Lanza, R. Bertazzoli, Effects of the Modification of Gas Diffusion Electrodes by Organic Redox Catalysts for Hydrogen Peroxide Electrosynthesis, J. Braz. Chem. Soc. 19 (2008) 643–650.

[25] F.L. Silva, R.M. Reis, W.R.P. Barros, R.S. Rocha, M.R.V. Lanza, Electrogeneration of hydrogen peroxide in gas diffusion electrodes: application of iron (II) phthalocyanine as a modifier of carbon black, J. Electroanal. Chem. 722–723 (2014) 32–37, https://doi.org/10.1016/j.jelechem.2014.03.007.
[26] R.M. Reis, A.A.G.F. Beati, R.S. Rocha, M.H.M.T. Assumpção, M.C. Santos, R. Bertazzoli, M.R.V. Lanza, Use of gas diffusion electrode for the in situ generation of hydrogen peroxide in an electrochemical flow-by reactor, Ind. Eng. Chem. Res. 51 (2012) 649–654, https://doi.org/10.1021/ie201317u.
[27] J.C. Forti, J.A. Nunes, M.R.V. Lanza, R. Bertazzoli, Azobenzene-modified oxygen-fed graphite/PTFE electrodes for hydrogen peroxide synthesis, J. Appl. Electrochem. 37 (2007) 527–532, https://doi.org/10.1007/s10800-006-9285-x.
[28] R.M. Reis, R.B. Valim, R.S. Rocha, A.S. Lima, P.S. Castro, M. Bertotti, M.R.V. Lanza, The use of copper and cobalt phthalocyanines as electrocatalysts for the oxygen reduction reaction in acid medium, Electrochim. Acta 139 (2014) 1–6, https://doi.org/10.1016/j.electacta.2014.07.003.
[29] M.H.M.T. Assumpção, R.F.B. De Souza, D.C. Rascio, J.C.M. Silva, M.L. Calegaro, I. Gaubeur, T.R.L.C. Paixão, P. Hammer, M.R.V. Lanza, M.C. Santos, A comparative study of the electrogeneration of hydrogen peroxide using Vulcan and Printex carbon supports, Carbon N. Y. 49 (2011) 2842–2851, https://doi.org/10.1016/j.carbon.2011.03.014.
[30] A. Moraes, M.H.M.T. Assumpção, F.C. Simões, V.S. Antonin, M.R.V. Lanza, P. Hammer, M.C. Santos, Surface and Catalytical effects on Treated Carbon Materials for Hydrogen Peroxide Electrogeneration, Electrocatalysis. 7 (2016) 60–69, https://doi.org/10.1007/s12678-015-0279-5.
[31] E. Yeager, The 1985 Berzelius Lecture, J. Mol. Catal. 38 (1986) 5–25.
[32] P.S. Guin, S. Das, P.C. Mandal, Electrochemical reduction of Quinones in different media: a review, Int. J. Electrochem. 2011 (2011) 1–22, https://doi.org/10.4061/2011/816202.
[33] B. Šljukić, C.E. Banks, S. Mentus, R.G. Compton, H. Inoue, S.R. Brankovic, J.X. Wang, R.R. Adzjic, Y. Zhang, S. Asahina, S. Yoshihara, S. Shirakashi, S.M. Golabi, J.B. Raoof, D. van den Ham, C. Hinnen, G. Magner, M. Savyf, M. Shamsipur, A. Salimi, H. Haddadzadeh, M.F. Mousavi, E. Katz, H.L. Schmidt, M.-C. Pham, J.-E. Dubois, M.S. El-Deab, T. Ohsaka, J. Yang, J.J. Xu, I. Bhugun, F.C. Anson, S.-J. Liu, C.-H. Huang, C.-C. Chang, K. Vaik, D.J. Schiffrin, K. Tammeveski, A. Salimi, C.E. Banks, R.G. Compton, A. Salimi, H. Eshghi, H. Sharghi, S.M. Golabi, Y. Usui, K. Sato, M. Tanaka, C.E. Banks, R.G. Compton, C.E. Banks, R.G. Compton, M.E. Abdelsalam, P.R. Birkin, M.A. Margulius, A.N. Mal'tsev, M.A. Margulis, I.M. Margulis, P. Tissot, A. Huissoud, C.P. Andrieux, J.M. Savéant, J. Koutecky, V.G. Levich, Modification of carbon electrodes for oxygen reduction and hydrogen peroxide formation: The search for stable and efficient sonoelectrocatalysts, Phys. Chem. Chem. Phys. 6 (2004) 992–997, https://doi.org/10.1039/B316412H.
[34] J.F. Carneiro, R.S. Rocha, P. Hammer, R. Bertazzoli, M.R.V. Lanza, Hydrogen peroxide electrogeneration in gas diffusion electrode nanostructured with Ta2O5, Appl. Catal. A Gen. 517 (2016) 161–167, https://doi.org/10.1016/j.apcata.2016.03.013.
[35] J.F. Carneiro, M.J. Paulo, M. Siaj, A.C. Tavares, M.R.V. Lanza, Nb2O5nanoparticles supported on reduced graphene oxide sheets as electrocatalyst for the H2O2electrogeneration, J. Catal. 332 (2015) 51–61, https://doi.org/10.1016/j.jcat.2015.08.027.
[36] W.R.P. Barros, Q. Wei, G. Zhang, S. Sun, M.R.V. Lanza, A.C. Tavares, Oxygen reduction to hydrogen peroxide on Fe3O4 nanoparticles supported on Printex carbon and Graphene, Electrochim. Acta 162 (2015) 263–270, https://doi.org/10.1016/j.electacta.2015.02.175.
[37] J.F. Carneiro, M.J. Paulo, M. Siaj, A.C. Tavares, M.R.V. Lanza, Zirconia on reduced graphene oxide sheets: synergistic catalyst with high selectivity for H2O2 electrogeneration, ChemElectroChem 4 (2017) 508–513, https://doi.org/10.1002/celc.201600760.
[38] J.F. Carneiro, L.C. Trevelin, A.S. Lima, G.N. Meloni, M. Bertotti, P. Hammer, R. Bertazzoli, M.R.V. Lanza, Synthesis and characterization of ZrO2/C as electrocatalyst for oxygen reduction to H2O2, Electrocatalysis 8 (2017) 189–195, https://doi.org/10.1007/s12678-017-0355-0.
[39] M.H.M.T. Assumpção, A. Moraes, R.F.B. De Souza, M.L. Calegaro, M.R.V. Lanza, E.R. Leite, M.A.L. Cordeiro, P. Hammer, M.C. Santos, Influence of the preparation method and the support on H2O2 electrogeneration using cerium oxide nanoparticles, Electrochim. Acta 111 (2013) 339–343, https://doi.org/10.1016/j.electacta.2013.07.187.
[40] M.H.M.T. Assumpão, A. Moraes, R.F.B. De Souza, I. Gaubeur, R.T.S. Oliveira, V.S. Antonin, G.R.P. Malpass, R.S. Rocha, M.L. Calegaro, M.R.V. Lanza, M.C. Santos, Low content cerium oxide nanoparticles on carbon for hydrogen peroxide electrosynthesis, Appl. Catal. A Gen. 411–412 (2012) 1–6, https://doi.org/10.1016/j.apcata.2011.09.030.
[41] A. Moraes, M.H.M.T. Assumpção, R. Papai, I. Gaubeur, R.S. Rocha, R.M. Reis, M.L. Calegaro, M.R.V. Lanza, M.C. Santos, Use of a vanadium nanostructured material for hydrogen peroxide electrogeneration, J. Electroanal. Chem. 719 (2014) 127–132, https://doi.org/10.1016/j.jelechem.2014.02.009.
[42] V.S. Antonin, M.H.M.T. Assumpção, J.C.M. Silva, L.S. Parreira, M.R.V. Lanza, M.C. Santos, Synthesis and characterization of nanostructured electrocatalysts based on nickel and tin for hydrogen peroxide electrogeneration, Electrochim. Acta 109 (2013) 245–251, https://doi.org/10.1016/j.electacta.2013.07.078.
[43] N. Guillet, L. Roué, S. Marcotte, D. Villers, J.P. Dodelet, N. Chhim, S. Trévin, Electrogeneration of hydrogen peroxide in acid medium using pyrolyzed cobalt-based catalysts: Influence of the cobalt content on the electrode performance, J. Appl. Electrochem. 36 (2006) 863–870, https://doi.org/10.1007/s10800-005-7174-3.
[44] U.A. Paulus, T.J. Schmidt, H.A. Gasteiger, R.J. Behm, Oxygen reduction on a high-surface area Pt / Vulcan carbon catalyst: a thin-film rotating ring-disk electrode study Oxygen reduction on a high-surface area Pt / Vulcan carbon catalyst: a thin-film rotating ring-disk electrode study, J. Electroanal. Chem. 495 (2014) 134–145, https://doi.org/10.1016/S0022-0728(00)00407-1.
[45] B. Šljukić, C.E. Banks, R.G. Compton, An overview of the electrochemical reduction of oxygen at carbon-based modified electrodes, J. Iran. Chem. Soc. 2 (2005) 1–25, https://doi.org/10.1007/BF03245775.
[46] R.S. Rocha, R.M. Reis, A.A.G.F. Beati, M.R.V. Lanza, M.D.P.T. Sotomayor, R. Bertazzoli, Desenvolvimento e avaliação de eletrodos de difussão gasosa (EDG) para geração de H2O2 in situ e sua aplicação na degradação do corante reativo azul 19, Quim. Nova 35 (2012) 1961–1966, https://doi.org/10.1590/S0100-40422012001000014.
[47] C.B. Solomons, T.W.G. Fryhle, Organic Chemistry, 10th ed., (2011).
[48] G.A. Kolyagin, V.L. Kornienko, The effect of carbon black mixture composition on the structural and electrochemical characteristics of gas diffusion electrodes for electrosynthesis of hydrogen peroxide, Russ. J. Electrochem. 52 (2016) 185–191, https://doi.org/10.1134/S1023193516020063.
[49] C.M. Long, M.A. Nascarella, P.A. Valberg, Carbon black vs. black carbon and other airborne materials containing elemental carbon: physical and chemical distinctions, Environ. Pollut. 181 (2013) 271–286, https://doi.org/10.1016/j.envpol.2013.06.009.
[50] E. Santacesaria, M. Di Serio, A. Russo, U. Leone, R. Velotti, Kinetic and catalytic aspects in the hydrogen peroxide production via anthraquinone, Chem. Eng. Sci. 54 (1999) 2799–2806, https://doi.org/10.1016/S0009-2509(98)00377-7.
[51] T. Nishimi, T. Kamachi, K. Kato, T. Kato, K. Yoshizawa, Mechanistic study on the production of hydrogen peroxide in the anthraquinone process, Eur. J. Org. Chem. (2011) 4113–4120, https://doi.org/10.1002/ejoc.201100300.
[52] G.R. Agladze, G.S. Tsurtsumia, B.I. Jung, J.S. Kim, G. Gorelishvili, Comparative study of hydrogen peroxide electro-generation on gas-diffusion electrodes in undivided and membrane cells, J. Appl. Electrochem. 37 (2007) 375–383, https://doi.org/10.1007/s10800-006-9269-x.
[53] R. Rocha, A.A.G.F. Beati, J.G. Oliveira, M.R.V. Lanza, Avaliação da degradação do diclofenaco sódico utilizando H2 o2 /fenton em reator eletroquímico, Química Nova 32 (2009) 354–358.
[54] W.R.P. Barros, S.A. Alves, P.C. Franco, J.R. Steter, R.S. Rocha, M.R.V. Lanza, Electrochemical Degradation of Tartrazine Dye in Aqueous Solution Using a Modified Gas Diffusion Electrode, J. Electrochem. Soc. 161 (2014) H438–H442, https://doi.org/10.1149/2.015409jes.
[55] W.R.P. Barros, P.C. Franco, J.R. Steter, R.S. Rocha, M.R.V. Lanza, Electro-Fenton degradation of the food dye amaranth using a gas diffusion electrode modified with cobalt (II) phthalocyanine, J. Electroanal. Chem. 722–723 (2014) 46–53, https://doi.org/10.1016/j.jelechem.2014.03.027.
[56] R.S. Rocha, F.L. Silva, R.B. Valim, W.R.P. Barros, J.R. Steter, R. Bertazzoli, M.R.V. Lanza, Effect of Fe2 +on the degradation of the pesticide profenofos by electrogenerated H2O2, J. Electroanal. Chem. 783 (2016) 100–105, https://doi.org/10.1016/j.jelechem.2016.11.038.